© 2018. This manuscript version is made available under the CC-BY-NC-ND 4.0 license
http://creativecommons.org/licenses/by-nc-nd/4.0/

Auxiliary consumption: a necessary energy that affects thermoelectric generation

P. Aranguren[1,2*], M. Araiz[1,2], D. Astrain[1,2],

[1] *Mechanical, Energy and Materials Engineering Department Public University of Navarre, 31006 Pamplona, Spain*

[2] *Smart Cities Institute, Pamplona, Spain*

[*] *e-mail:patricia.arangureng@unavarra.es*

Keywords: water cooling; auxiliary consumption; thermoelectric generation; optimization; waste heat harvesting

Abstract

Waste heat recovery can apply to a wide range of applications, from transportation, or industries to domestic applications. The attempts to increase the efficiency of thermoelectric generators to make this technology appealing for waste heat harvesting include the study of novel heat exchangers to be located at the generators. A liquid cooling fluid presents high heat transfer coefficients. However, it needs a pump to make it circulate through the system. Besides, to have a constant input of fresh refrigerant, the dissipation systems need secondary heat exchangers to cool down the refrigerant, so as it can be reused again. A computational methodology, which simulates the behavior of thermoelectric generators has been used to determine the potential of waste heat harvesting. The optimal thermoelectric energy obtained using heat dissipation systems with liquid as the heat-carrier is 119 MWh/year, while the maximum net energy, the usable energy, is 73 MWh/year due to the consumption of the auxiliary equipment. The latest value does represent not only a 40 % reduction from the optimal thermoelectric

generation but also a different optimal working point. The complete elimination of the auxiliary equipment at this application could produce up to 128 MWh/year.

Nomenclature

δ	Occupancy ratio	
ρ_l	Density of the water	Kg/m^3
Δp_{CP}	Hydraulic losses of the cold plate	kPa
Δp_f	Hydraulic losses of the fan-coil	kPa
Δp_{23}	Hydraulic losses of the refrigeration system between the exit of the cold plate and the entry of the fan-coil	kPa
Δp_{41}	Hydraulic losses of the refrigeration system between the exit of the fan-coil and the entry of the cold plate	kPa
η_{pump}	Efficiency of the pump	
A_{TEM}	Area of a TEM	m^2
A_{dis}	Available dissipative area	m^2
M_{TEM}	Number of TEMs	
$\dot{m}_a$	Mass flow of the air	kg/s
$\dot{m}_{gas}$	Mass flow of the flue gases	kg/s
$\dot{m}_l$	Mass flow of the refrigerant liquid	kg/s
$\dot{Q}_C$	Calorific power to dissipate	W
$\dot{Q}_{CP}$	Calorific power dissipated by the cold plate	W
$\dot{Q}_f$	Calorific power dissipated by the fan-coil	W
$\dot{Q}_{23}$	Calorific power dissipated by the refrigeration system between the exit of the cold plate and the entry of the fan-coil	W

$\dot{Q}_{41}$	Calorific power dissipated by the refrigeration system between the exit of the fan-coil and the entry of the cold plate	W
R_C^{TEM}	Thermal resistance of the heat exchanger located on the cold side per thermoelectric module	K/W
R_C	Thermal resistance of the heat exchanger located on the cold side	K/W
R_{CP}	Thermal resistance of the cold plate	K/W
T_1	Temperature at the entry of the cold plate	K
T_2	Temperature at the exit of the cold plate	K
T_3	Temperature at the entry of the fan-coil	K
T_4	Temperature at the exit of the fan-coil	K
T_{amb}	Ambient temperature	K
T_{CP}	Temperature of the cold plate	K
U	Overall heat transfer coefficient	W/m^2K
$\dot{W}_{aux}$	Consumption of the auxiliary equipment	W
$\dot{W}_{fan}$	Electrical consumption of the fans	W
$\dot{W}_{pump}$	Electrical consumption of the pump	W
$\dot{W}_{TEM}$	Thermoelectric generation	W
$\dot{W}_{net}$	Net generation	W

1. Introduction

Despite the gratuity of waste heat, the low efficiency that thermoelectric generation presents is a deterrent for the applicability and profitability of big scale systems. Thus, great efforts to improve the efficiency of thermoelectric generators (TEGs) are being made. The two most important actions are the improvement of the thermoelectric

materials and the thermal optimization of the TEG as a whole. To fulfill the latter aspect new different types of heat exchangers are nowadays studied aiming to reduce the thermal resistances on both sides of the thermoelectric modules (TEMs), as they would procure higher thermoelectric generation [1,2]. One of the approaches is to include liquid refrigerants into the heat dissipation systems to improve the thermal resistances [3–5]. Due to their heat transfer coefficients their thermal resistances are good, however extra power consumption is needed since a pump is required to make the refrigerant circulate along the circuit. Thus, to optimize the net generation (the thermoelectric generation minus the consumption of the auxiliary equipment), the increase on thermoelectric generation and the increment of the auxiliary consumption have to be born in mind [6,7]. The effect of longitudinal vortex generators and the introduction of inserts or metal foams enhance heat transfer, but they provoke higher pressure drops, and hence the consumption of the pumps greatly increases [6,8–10]. The increase in thermoelectric generation could not be as noticeable as the growth in the auxiliary consumption, obtaining lower net generations [6,11,12], a totally non-desirable scenario.

Moreover, most of the studies of the literature do not take into account the necessity of reducing the temperature of the refrigerant. Due to the heat absorbed by the fluids when they circulate through the heat exchangers, their temperature increases. Therefore, the temperature of the refrigerants needs be lowered for continuous operation. The dissipator in charge of decreasing the temperature of the fluid increases the thermal resistance of the refrigeration system, worsening the thermoelectric generation. Besides, this exchanger could include auxiliary equipment, hence extra consumption needs to be redrawn from the thermoelectric generation [13,14].

To complete eliminate the auxiliary equipment, novel heat exchangers are used where the fluid circulates thanks to phase change and sometimes gravity. These devices improve

even more the heat transfer due to the use of the latent heat of the internal fluid [15]. The fluid evaporates due to the heat absorbed at the evaporator. It flows up to the condenser, where it releases heat to the ambient and condensates. Finally, the liquid returns to the evaporator closing the loop. Thermosyphons could eliminate the necessity of including any auxiliary equipment if they present free convection with the ambient, however as they lack of wick, they need to work vertically so gravity brings back the condensed fluid to the evaporator [16]. Many novel applications are including these devices into TEGs, variable conductance heat pipe/thermosiphon allow the TEG to work at constant hot face temperature during a driving cycle [17], waste heat recovery using heat pipes and TEG to produce electricity [18] or power generation from solar ponds using combined thermosiphon and TEGs [19].

The optimization of the thermal design of TEGs is essential to improve their efficiency. Not only the heat exchangers and their mass flows have to be optimized, but also the number of TEMs used. The occupancy ratio (equation (1)), determines the thermoelectric generation. A higher number of TEMs seems to produce higher thermoelectric generation, but as the thermal resistance per TEM of each heat exchanger worsens, it is not always true that a bigger δ produces higher thermoelectric generation [20–22].

$$\delta = \frac{M_{TEM} A_{TEM}}{A_{dis}} \tag{1}$$

This paper studies two dissipators: a heat dissipation system with water as the heat-carrier and a thermosyphon that refrigerate a TEG located at the exhaust of a real furnace. To that purpose, a general methodology makes two validated computational models [13,23] interact to optimize the net thermoelectric generation modifying the occupancy ratio, the mass flow of the refrigerants and the consumption of the auxiliary equipment. The influence on the net generation of including the secondary heat exchanger in charge of reducing the temperature of the water and the auxiliary consumption is quantified,

highlighting the fact that those influences are not negligible and should be taken into account for the design of TEG systems.

2. Thermoelectric generation optimization methodology

TEG systems produce electric energy out of temperature gradients. TEGs can be applied to any application where a difference of temperature exists, however, applications, where waste heat exists, are very promising, as waste heat is costless and it appears at any application. To optimize the net thermoelectric generation (equation (2)) two validated computational models interact and seek the optimal working point. One computational model simulates the thermal resistance of the dissipation system with liquid as the heat-carrier (Refrigeration System computational model (RS model)) and obtains the consumption of the auxiliary equipment (equation (3)) [13]. The second one simulates the thermoelectric generation of any application (Thermoelectric Generator computational model (TEG model)), but especially those which present waste heat conducted through a pipe to the ambient [23]. The whole methodology includes the occupancy ratio, the mass flow of the refrigerants, the calorific power to dissipate and the temperature variation of the heat source.

$$\dot{W}_{net} = \dot{W}_{TEM} - \dot{W}_{aux} \tag{2}$$

$$\dot{W}_{aux} = \dot{W}_{pump} + \dot{W}_{fan} \tag{3}$$

Figure 1 presents the methodology to compute the net thermoelectric generation of any application, especially those applications where electric energy is obtained from waste heat emitted as flue gases to the atmosphere. The presented interaction includes heat exchangers with liquid as the heat-carrier on the cold side of the generators, but the same methodology could be used to obtain the generation of any system involving any other kind of heat dissipators.

The RS model obtains the thermal resistance of the heat exchanger as a function of the calorific power to dissipate, an output of the thermoelectric generation model. To solve this aspect, firstly the calorific power is estimated to obtain the thermal resistance, a necessary input for the TEG model. The latter computational model solves the thermoelectric phenomena and obtains the calorific power dissipated by the cold side heat exchanger, the new value that closes the iteration loop. Once the solution is reached, the thermoelectric generation is obtained and given the consumption of the auxiliary equipment; the net generation is computed, the parameter to optimize.

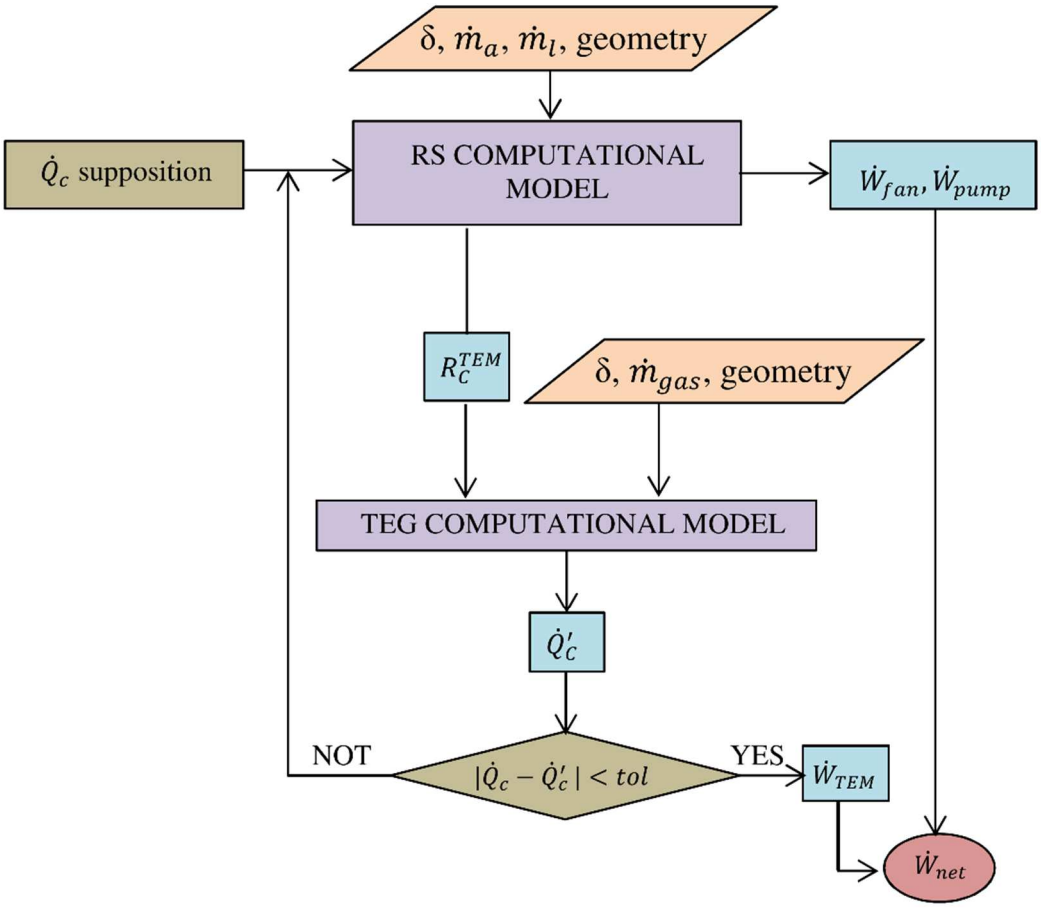

Figure 1. Interaction between the refrigeration system and the thermoelectric generation computational model

a. Thermoelectric Generator computational model

This model is specially developed for applications where TEGs harvest heat from flue gases which flow along a pipe. This model includes the temperature drop of the flue gases while they exchange heat with the TEG system, a significant variable variation as the thermoelectric generation of a built prototype was reduced by a 65 % due to the temperature drop of the gases between two different levels. The error of this computational model is the ±12 % [23].

The TEG computational model uses the finite differences method to solve the thermoelectric phenomena. Moreover, this model includes each component of the system: the contacts, the ceramics of the TEMs, each thermoelectric effect, novel parameters such as the mass flow of the refrigerants, the occupancy ratio and the temperature decrease of the flue gases, as well as it takes into account the temperature dependence of the thermoelectric properties, and it solves the transient state.

The TEG computational model needs the thermal resistances of the different elements of the generator to calculate the thermoelectric generation. Including heat exchangers with fluid as the heat-carrier into a TEG improves the thermoelectric generation, but the net generation has to be computed, as it is not that trivial to assure that in any case, the incorporation of this kind of heat dissipators is right for this generation. Hence a refrigeration system computational model is developed and included in the calculation methodology.

b. Refrigeration system computational model

The use of a heat exchanger with liquid as a heat-carrier to dissipate the heat emitted by a TEG involves the inclusion of extra elements, such as a pump to drive the fluid and a secondary heat exchanger to cool down the refrigerant to be reused again. Figure 2 presents a conventional heat dissipation system located on the cold side of a TEM. The heat to be dissipated ($\dot{Q}_C$) is absorbed by the refrigerant fluid which is driven through the

whole circuit by the pump. The secondary heat exchanger cools down the temperature of the refrigerant. This heat dissipator normally transfers heat to the surrounding air and it is commonly provided with a fan to improve the convection with the ambient.

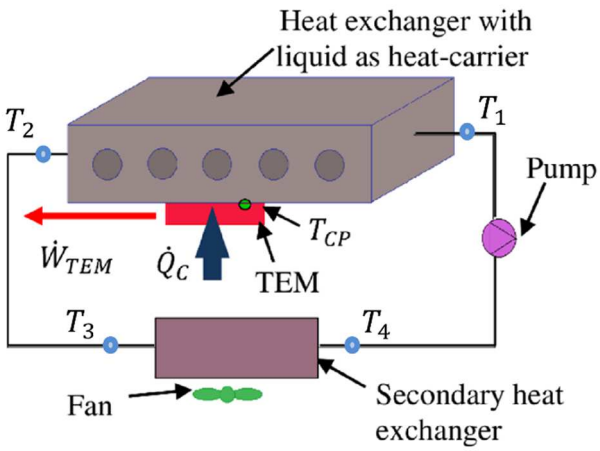

Figure 2. Heat dissipation system including a heat exchanger with liquid as the heat-carrier [14]

A computational methodology, which includes influential parameters such as the occupancy ratio (δ), the mass flow of the refrigerants ($\dot{m}_a$,$\dot{m}_l$) and the calorific power to dissipate ($\dot{Q}_C$) was developed to characterize the thermal resistance per TEM of the whole refrigeration system [13]. This model presents an accuracy of the 93 % and its schematic can be consulted in Figure 3.

A range of mass flows are simulated in order to obtain the working point of the refrigeration system, The upper limit of the mass flow is denoted as M and can be selected by the user. Within each mass flow, the computational model calculates the heat transfer coefficients (U) of the different elements of the system through an iteration loop using the entry and exit temperatures of the cold plate and fan-coil (T_1, T_2, T_3 and T_4) and the pressure drops are obtained to calculate the working point of the system, obtaining the thermal resistance of the system and the consumption of the auxiliary equipment.

The thermal resistance per TEM of the whole refrigeration system is defined by equation (4). The temperature difference between the cold plate and the ambient is divided by the calorific power dissipated and the number of TEMs. This thermal resistance includes the thermal resistance of the heat exchanger located on the cold side of the TEMs, known as a cold plate, the resistance of the secondary heat exchanger and that of the pipes and the rest of the devices involved in the refrigeration system. The auxiliary consumption of the fan of the secondary heat exchanger as well as the consumption of the pump are included into the total auxiliary consumption (equation (2)), the electrical power to be redrawn from the thermoelectric generation to obtain the usable electrical generation ($\dot{W}_{net}$) expressed in equation (1).

$$R_C^{TEM} = \frac{T_{CP} - T_{amb}}{\dot{Q}_C / M_{TEM}} \tag{4}$$

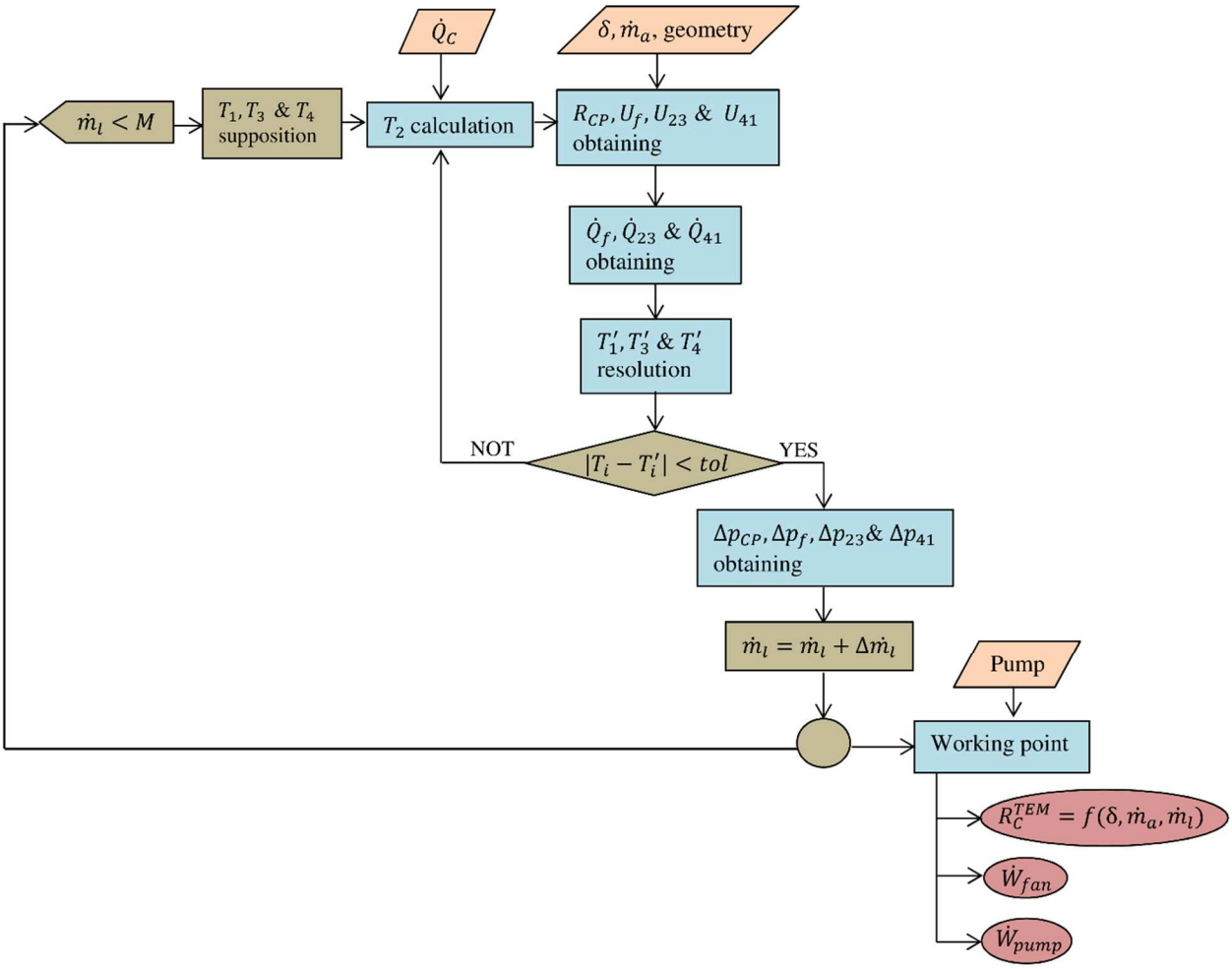

Figure 3. Schematic of the computational model that obtains the thermal resistance of the heat dissipation system [13]

3. Optimization study

To estimate the potential of the optimization methodology a real Spanish industry has been selected. The consumption of thermal energy of this industry is massive, as it includes ceramic cooking processes. Its waste heat, as high-temperature smoke emitted to the ambient through the chimney, can be easily harvested through TEGs. The chimney has a height of 12 m and a diameter of 0.8 m, a total of 33.6 m^2 to locate the thermoelectric generator, while the flue gases have a mass flow of $\dot{m}_{gas}$ =5.49 kg/s and a temperature of 187 ºC. The ambient temperature is selected as T_{amb}=17 ºC, the mean temperature of the area where the industry is.

Every element has to be defined through its thermal resistance and heat capacity as Figure 2 depicts. The thermoelectric modules simulated are TG12-8-01-L from Marlow Industries, which support up to 250 ºC on one of their sides due to special welding [24]. Their properties define their particularities. The hot side heat exchanger is selected to be a finned dissipator with a fin spacing of 10 mm, a fin high of 50 mm and a fin thickness of 1.5 mm. The base thickness is 4mm, and the finned dissipator is located in the interior of the chimney. To get the thermal resistance of the heat dissipator a CFD software was used, ANSYS Fluent. The influence of the occupancy ratio, as well as the velocity of the flue gases, have been evaluated, as Figure 4 depicts. The tendencies are similar, a higher number of TEMs (higher occupancy ratios) present higher thermal resistances, due to the reduction of the effective dissipative area per TEM, and higher velocities (higher mass flow rates) procure smaller thermal resistances since the heat transfer coefficients improve.

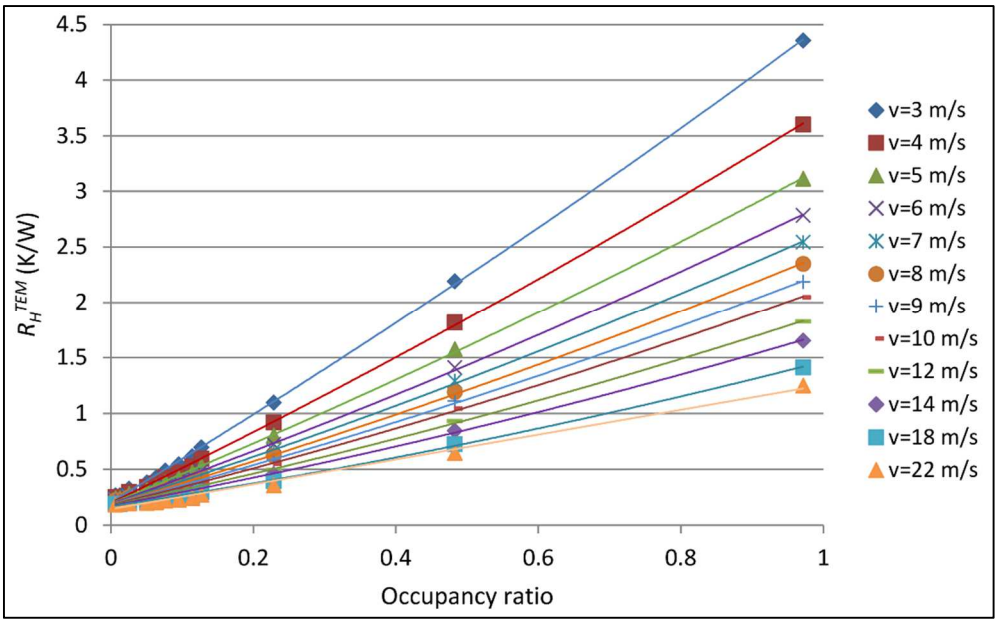

Figure 4. Thermal resistance per thermoelectric module of the finned dissipator located on the hot side of the TEG as a function of the occupancy ratio and the velocity of the flue gases

a. Cold side heat exchanger thermal characterization

The RS computational model is used to characterize the cold side heat exchanger thermally. The dissipation system is mainly composed of a cold plate formed by 6.2 mm parallel channels separated 3 mm, a fan-coil provided with 8 mm copper tubes, longitudinal fins with a thickness of 0.2 mm and separated 1.6 mm provided with fans that make the air circulate through its fins and a pump that makes the water circulate along the circuit. The cold plate is located on the hot side of the TEMs while the fan-coil is located at the bottom of the chimney, where the water is cooled down to be reused again. The thermal characterization has been done modifying four parameters: the calorific power to dissipate ($100<\dot{Q}_C<500$ W), the occupancy ratio ($0.073<\delta<0.625$), the water mass flow ($0.024<\dot{m}_l<0.055$ kg/s) and the air mass flow along the fan-coil ($0.090<\dot{m}_a<0.243$ kg/s).

Figure 5 presents the influence of the calorific power to dissipate on the thermal resistance by TEM of the dissipation system for different air mass flows. As the figure depicts, the range of calorific powers simulated slightly influences the thermal resistance as the calorific power to dissipate influences the temperature of the water that circulates through the system. Due to its high specific heat, the maximum difference in temperature is 4 ºC, a very small temperature difference to cause significant changes in the heat transfer coefficients, and thus on the thermal resistance of the system. Even though there is a decreasing tendency, the slope is so small as to neglect the influence of the calorific power to dissipate on the thermal resistance per TEM of the system.

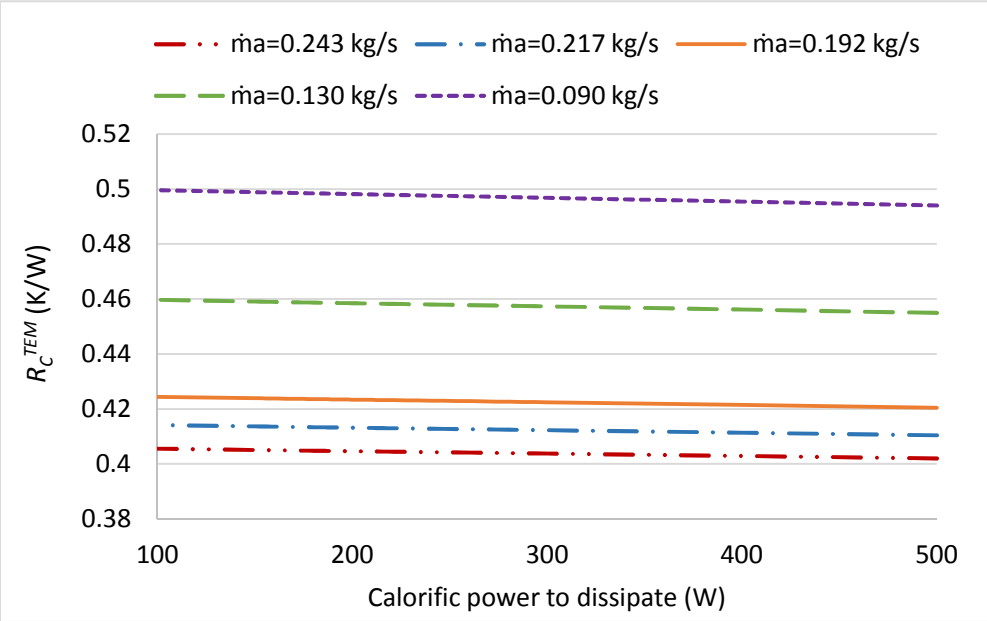

Figure 5. Thermal resistance per TEM of the dissipation system with liquid as the heat-carrier as a function of the calorific power to dissipate and the air mass flow for a constant water mass flow of $\dot{m}_l = 0.055$ kg/s.

Figure 6 and Figure 7 present the influence of the occupancy ratio (the number of TEMs installed) and the mass flow of the refrigerants on the thermal resistance of the refrigeration system. As the occupancy ratio increases, adding more TEMs, the thermal resistance per TEM increases. The increment of the number of TEMs means a reduction

in the effective dissipative area devoted to each TEM, and thus an increase in the thermal resistance. Therefore, an increase of δ does not always mean an increment on the thermoelectric generation, as it will be analyzed later on.

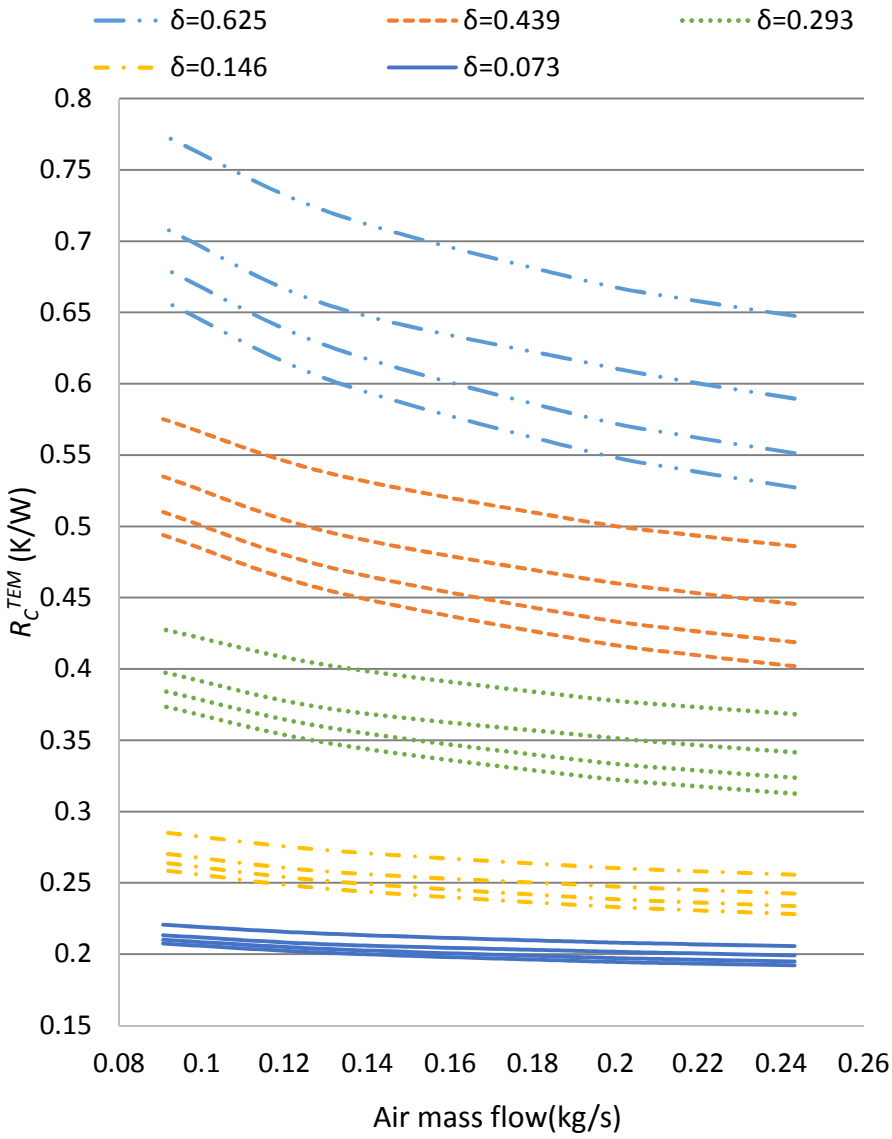

Figure 6. Thermal resistance per TEM of the dissipation system with liquid as the heat-carrier as a function of the occupancy ratio and the air and water mass flows. $\dot{m}_l$=0.024; 0.035; 0.044 and 0.055 kg/s.

The four different curves of each occupancy ratio that can be seen in Figure 8 correspond to the four different water mass flows simulated ($\dot{m}_l$=0.024; 0.035; 0.044 and 0.055 kg/s),

the biggest water mass flow is represented by the bottom curve while the smallest by the upper one of each δ. The mass flow of the air highly influences the thermal resistance of the system for high occupancy ratios, whereas when small occupancy ratios the influence is less significant. High occupancy ratios procure small effective dissipative areas per TEM. Hence, an improvement of the heat transfer coefficients, through the increment of the refrigerant mass flows, greatly influences the thermal resistance. Figure 9 presents the same tendency for the water mass flow for different occupancy ratios. The surfaces of the smallest δ are practically horizontal, while the biggest occupancy ratios surfaces present a wider range of thermal resistances.

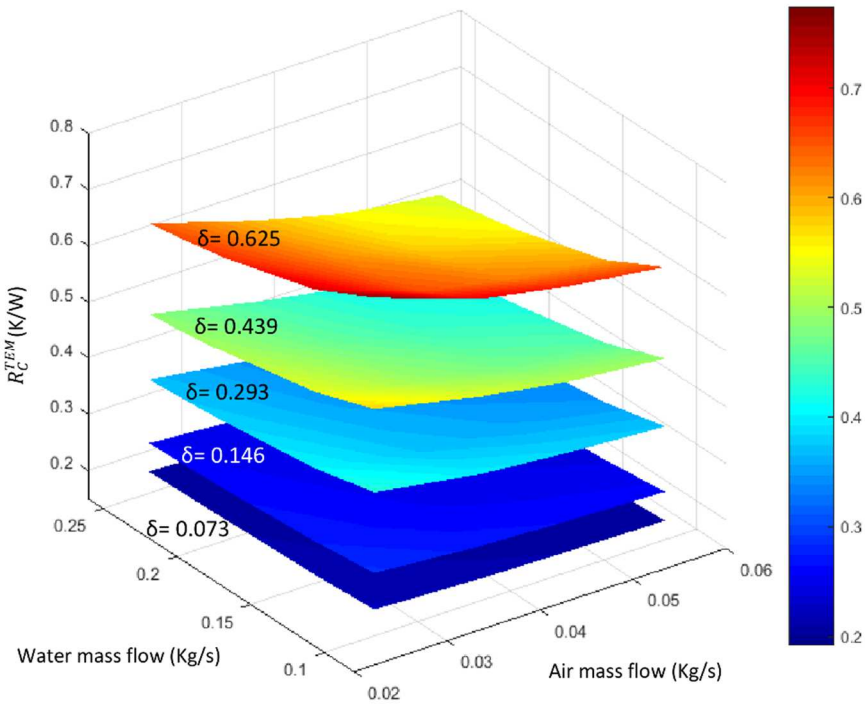

Figure 7. 3D plot of the influence of the occupancy ratio and the refrigerant mass flows on the thermal resistance of the refrigeration system per TEM

The occupancy ratio (δ) and the refrigerant mass flows ($\dot{m}_a, \dot{m}_l$) are factors that determine the thermal resistance per TEM of the refrigeration system with water as the heat-carrier as Figure 6 and Figure 7 present. However, the calorific power to dissipate ($\dot{Q}_C$) is not

influential as Figure 7 depicts. The thermal resistances of the heat exchangers are decisive for the thermoelectric generation, thus these parameters are going to be introduced into the general computational methodology to maximize the net thermoelectric generation.

b. Net thermoelectric generation

Figure 8 shows the thermoelectric generation as a function of the occupancy ratio and the mass flows of the refrigerants, the water that circulates through the system and the air that helps to refrigerate the water at the fan-coil. This figure presents the importance of selecting the optimal occupancy ratio as the maximum thermoelectric generation occurs when δ=0.439 (when the 43.9 % of the surface of the chimney is covered by TEMs), producing 14156 W. The thermal resistance of the heat dissipation systems worsens if the occupancy ratio increases, thus even a higher number of TEMs seems to provide higher generation, as each module is producing less power the total generation could decrease, as it happens for occupancy ratios greater than 0.439. The thermoelectric generation rises with the increase of both mass flows of the refrigerants. Higher mass flows procure better thermal resistance, thus the difference in temperature between the hot and the cold sides of the TEMs increase, producing more electric power.

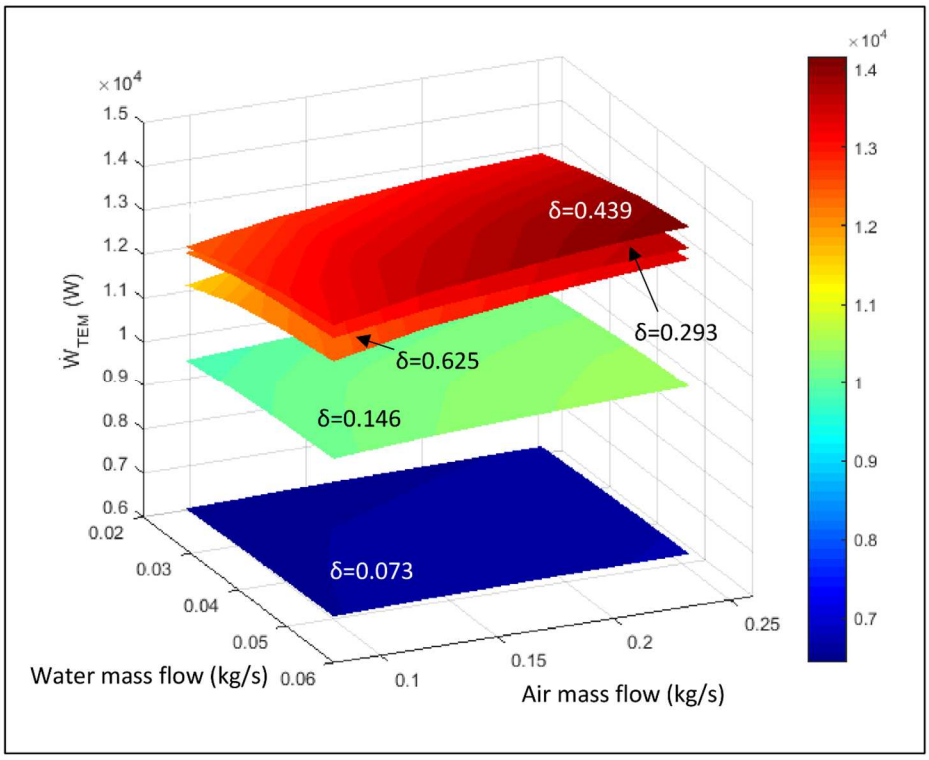

Figure 8. Thermoelectric generation as a function of the mass flow of the refrigerants and the occupancy ratios

Nevertheless, the increasing tendency of the thermoelectric generation with the increasing of the mass flow of the refrigerants is not represented in Figure 9. The latter figure presents the net generation, the thermoelectric generation minus the consumption of the auxiliary equipment, as a function of the mass flows of the refrigerants and the occupancy ratio. The maximum net generation equals 8703 W, and it is found around an occupancy ratio of 0.4. The increase in the mass flow of the refrigerants does not provide the same tendency as with the thermoelectric generation. The net generation decreases if the mass flows increase. This reduction is obtained by the increase of the consumption of the auxiliary equipment, which negatively influences the net generation. The increase of the thermoelectric generation due to the increments on the mass flows is less pronounced that the increase of the consumption of the auxiliary equipment. Some of the scenarios present in Figure 11 are not desirable because the net generation is negative, meaning that the auxiliary consumption is higher than the thermoelectric generation.

The consumption of the auxiliary equipment has been calculated as the sum of the consumption of the pump and that of the fans located at the fan-coil. The consumption of the pump is obtained using equation (5) [25], where ΔP_{CP} stands for the pressure drop at the cold plate and the efficiency of the pump (η_{pump}) was selected to be the 80 %. To account for the consumption of the fans at the fan-coil, the total electric consumption of the fan-coil of the prototype defined by the air mass flow has been multiplied by 769, as 769 cold plates like the prototype one could fit on the surface of the chimney.

$$\dot{W}_{pump} = \frac{\Delta P_{CP}\, \dot{m}_l / \rho_l}{\eta_{pump}} \tag{5}$$

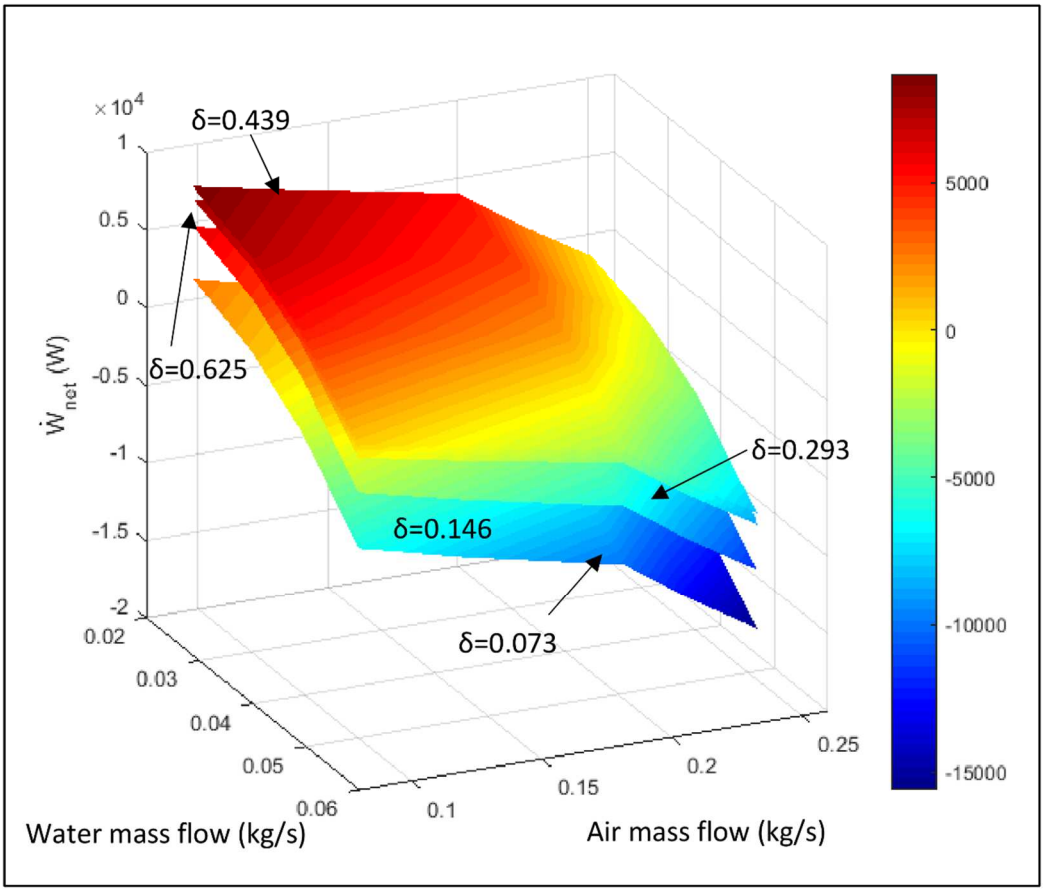

Figure 9. Net generation as a function of the mass flow of the refrigerants and the occupancy ratios

The influence of accounting for all the consumption of the auxiliary equipment is notorious. The maximum thermoelectric generation is 14156 W (119 MWh/year given

that the furnace works 350 days a year), while the maximum net generation is reduced by a 40 %, resulting in 8703 W (73 MWh/year). Besides, the optimum scenario is not anymore high refrigerant mass flows, but low ones as the consumption of the auxiliary equipment are smaller. The optimization of the working point is essential, as the net generation is drastically reduced if the working point is shifted.

Not to rely on the fan-coil, a second study is conducted assuming that the system is located by a water reservoir. Figure 10 includes the thermoelectric and net generations if the treatment of the water is not included, as the water is being continuosly taken from the water reservoir (a lake, the sea or a river). The thermoelectric generation is from an 8 to a 14 % higher if just the cold plate is simulated. This increase is due to the reduction of the thermal resistance of the system if the fan-coil is eliminated. Nevertheless, the biggest change corresponds to the net generation which highly increases if the fan-coil is eliminated from the refrigeration system. Increases of up to the 118 % can be found, a maximum net generation of 121 MWh/year around occupancy ratios of 0.4. Unlike the previous study, practically all the net generations are positive, meaning that the thermoelectric generation is higher than the consumption of the auxiliary equipment. There is just a small region - highest water mass flow and smallest occupancy ratio- where the net generation is negative due to the considerable consumption of the pump regarding the thermoelectric generation. For low occupancy ratios, the thermal resistances were barely dependent on the mass flow of the refrigerants. Thus high mass flows procure low net generations.

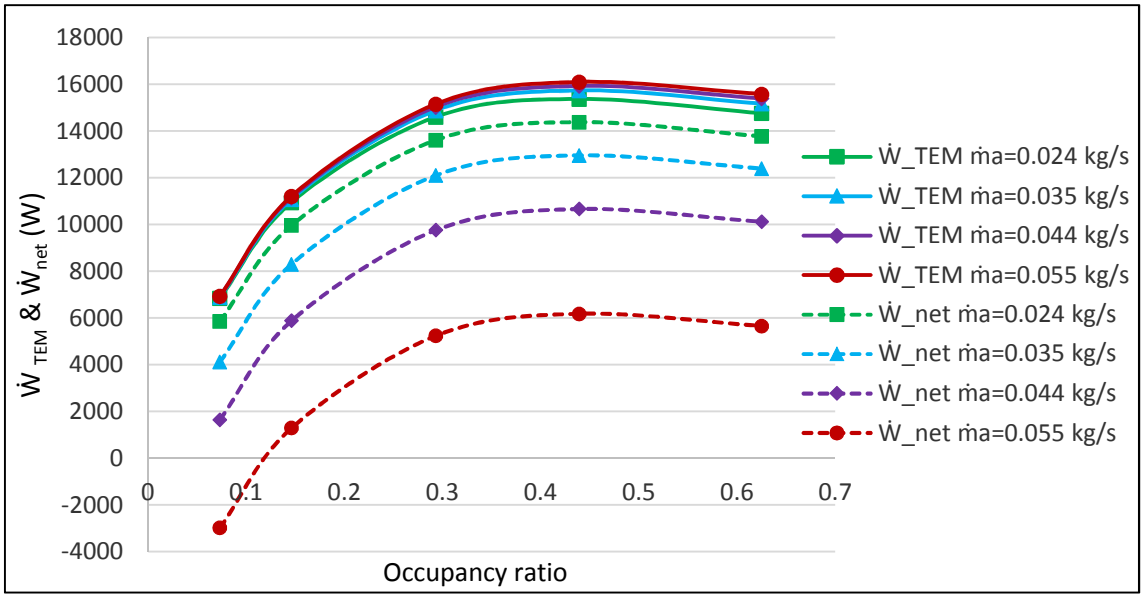

Figure 10. Net and thermoelectric generation of the cold plate as a function of the water mass flow and the occupancy ratio

The comparison between Figure 8, Figure 9 and Figure 10 present the great difference between the results if the treatment of the refrigerant is included into the calculations or not. Excluding the fan-coil, is feasible but the application must be nearby a water resource and sadly not many applications present this scenario. A cooling tower could be a good solution because it presents small electric consumption. Nevertheless, its installation requires a lot of space and a big investment, resulting in a non-attractive solution unless the TEG is installed into a big application provided with much free space. Between the maximum net generation of the first study (where the fan-coil and the consumption of its fans are taken into account) and the one from the second one (where no fan-coil is included), there could be different solutions as the consumption of the auxiliary equipment could be optimized. The consumption of the auxiliary equipment is a deterrent, as it shows the dramatic decrease in the net generation, hence it has to be taken into account.

4. Comparison with a novel technology

The thermal resistances of the heat exchangers which involve refrigerants are very low, producing high thermoelectric generations, however, as auxiliary equipment is necessary to make the system work, the net generation is not as appealing as we could have thought. Hence, a new dissipation system is studied, a phase change thermosyphon which includes a refrigerant that changes phase and naturally moves through the system thanks to gravity, meaning that no pump is needed. The fluid absorbs heat at the evaporator section, it evaporates and ascends to the condenser, once condensed it returns to the evaporator driven by the gravity force. To eliminate any auxiliary equipment, the condenser presents a significant area provided with extended surface as the heat transfer coefficients are low due to free convection.

A thermosyphon has been built and experimented to thermally characterize it as a function of the occupancy ratio and the calorific power to dissipate. Figure 11 presents its diagram, the hot plates simulate the heat flux that the system has to evacuate to the ambient. The evaporator absorbs the heat and the inside liquid evaporates. The vapor ascends to the condenser, where thanks to the extended surface it condenses and returns to the evaporator, closing the cycle. The condenser area is 6.92 m^2 and it is formed by 6 pipes, of 10 mm, distributed in 7 levels and crossed by longitudinal fins. The working fluid is R134a.

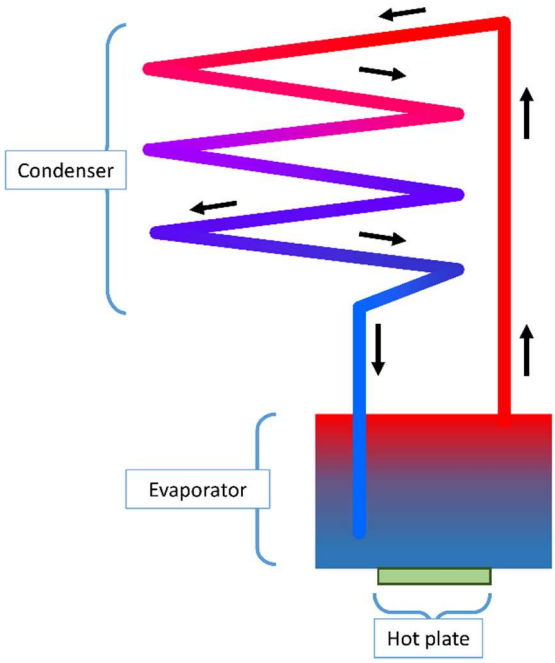

Figure 11. Thermosyphon diagram

Five values of occupancy ratios and six of calorific powers to dissipate have been selected to compute the thermal resistance. Three replicates have been made for each configuration to reduce the uncertainty. The thermal resistance has been calculated using equation (5), in this case T_{CP} stands for the temperature of the thermosyphon, T_{amb} is the ambient temperature and $\dot{Q}_C$ the calorific power to dissipate, this power is calculated multiplying the voltage and intensity supplied to the hot plates, whose size is similar to that of the TEMs. The overall uncertainty has been calculated using Coleman's work [26]. The temperature probes used present an uncertainty of ±0.5 ºC while the accuracy of the voltmeters and ammeters are ±0.2 V and ±0.02 A, respectively. The overall uncertainty in percentage is smaller than the 8.5 % in all cases.

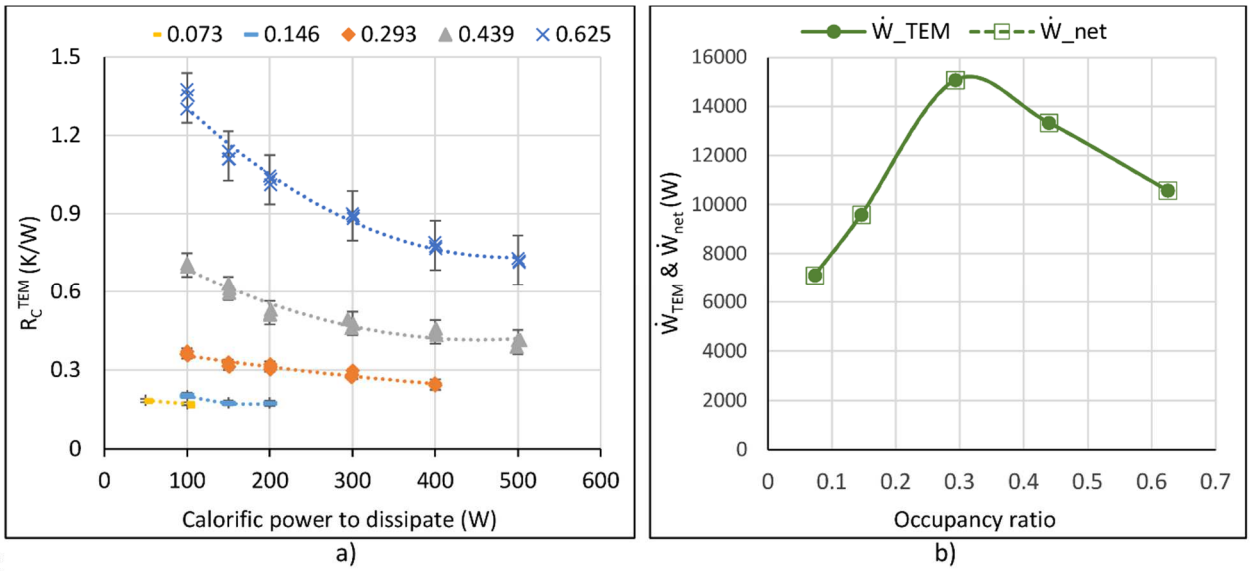

Figure 12. Thermosyphon, a) thermal resistance per TEM as a function of the calorific power to dissipate and the occupancy ratio, a) net and thermoelectric generation

Figure 12a) includes the thermal resistances of the thermosyphon along with their uncertainty. In this case, the thermal resistance depends on both, the occupancy ratio and the calorific power to dissipate. The increase of the calorific power to dissipate increases the temperature of the working fluid and thus the heat transfer inside the thermosyphon improves. Moreover, the free convection that takes place outside the heat dissipation system improves as the temperature difference between the ambient and the outer wall increases. Due to the previous facts, the influence of the calorific power to dissipate is that influential on the thermal resistance of the system, as Figure 12 a) presents.

The thermoelectric generation and the net generation have been computed using the general methodology shown previously for the real case of the Spanish industry. For the thermosyphons, the net generation is similar to the thermoelectric generation because there is no auxiliary consumption.

Comparing Figure 7 and Figure 12 a) it can be seen that the thermal resistances of the thermosyphon for high occupancy ratios and low calorific powers to dissipate are higher than that for the refrigeration system. Nevertheless, as the calorific power to dissipate

decreases, the thermal resistances considerably improve. The reduction of the thermal resistances obtains higher thermoelectric generations than for the refrigeration system with water, as Figure 12 b) shows. The optimal thermoelectric generation for the thermosyphons, which occurs around an occupancy ratio of 0.3, is 15200 W. As the thermosyphons do not need auxiliary equipment, the net generation corresponds with the thermoelectric one. Thus an annual energy of 128 MWh can be produced from the waste heat of a real Spanish Industry. This net generation is a 75 % higher than that of the refrigeration system with water and a 6 % higher than the net generation obtained if there is a water reservoir next to the dissipation system with a liquid as the heat-carrier.

The use of thermosyphons seems appealing. On the one hand, they operate by themselves, without any auxiliary consumption or the necessity of a water reservoir next to them. Nevertheless, on the other hand, they need a big surface area to assure that the fluid condensates by free convection and they need to be located vertically, so gravity brings back the condensates to the evaporator. Refrigeration systems with a liquid as the heat-carrier need a smaller space to be located on the chimney, and if necessary, the heat exchanger in charge of reducing the temperature of the refrigerant could be located outside the installation. Thus, if the application presents restricted space, or the refrigeration system cannot be found vertically, cold plates have to be used to refrigerate the TEG, a very interesting solution that has to take into account the consumption of the auxiliary equipment if the net generation wants to be optimized.

5. Conclusions

The computational methodology presents a net generation of 73 MWh/year if a TEG provided with a dissipation system with a fluid as the heat-carrier is installed in a real application, a furnace located in Spain. However, the net generation could be up to 121

MWh/year (a 66 % higher) if the application was installed nearby a natural resource of water.

All the applications where a TEG with dissipators including liquids as heat-carriers is installed require a secondary heat exchanger to treat the refrigerant unless being nearby a natural resource. The inclusion of a secondary heat exchanger, being in charge of reducing the temperature of the refrigerant, influences on two parameters. Firstly, the thermal resistance of the dissipation system is modified, as a reduction between the 8 and 14 % in the thermoelectric generation shows. Secondly, the secondary heat exchanger normally has auxiliary consumption that has to be taken into account. The studied case presents reductions in the net generation of up to the 118 %, just because of including the auxiliary consumption of the secondary heat exchanger. The thermoelectric generation is important, but much more is the net generation. Any application where TEGs are installed employ the net generation for other purposes, not the thermoelectric generation. Thus each component included into a TEG, and its auxiliary consumption has to be borne in mind when optimizing the application.

The installation of thermosyphons, which do not include any auxiliary equipment, produces a higher net generation, 128 MWh from the same application. Nevertheless, the surface that these systems need is very big and they have to operate vertically so that gravity can bring back the fluid to the evaporator.

Acknowledgments

The authors are indebted to the Spanish Ministry of Economy and Competitiveness for the economic support to this work, included in the DPI2014-53158-R research project.

References

[1] Wang Y, Dai C, Wang S. Theoretical analysis of a thermoelectric generator using exhaust gas of vehicles as heat source. Appl Energy 2013;112:1171–80.

doi:10.1016/j.apenergy.2013.01.018.

[2] Wang X, Li B, Yan Y, Liu S, Li J. A study on heat transfer enhancement in the radial direction of gas flow for thermoelectric power generation. Appl Therm Eng 2016;102:176–83. doi:10.1016/j.applthermaleng.2016.03.063.

[3] Zhou M, He Y, Chen Y. A heat transfer numerical model for thermoelectric generator with cylindrical shell and straight fins under steady-state conditions. Appl Therm Eng 2014;68:80–91. doi:10.1109/IWECA.2014.6845673.

[4] Zheng XF, Liu CX, Yan YY, Wang Q. A review of thermoelectrics research - Recent developments and potentials for sustainable and renewable energy applications. Renew Sustain Energy Rev 2014;32:486–503. doi:10.1016/j.rser.2013.12.053.

[5] Wang Y, Li S, Zhang Y, Yang X, Deng Y, Su C. The influence of inner topology of exhaust heat exchanger and thermoelectric module distribution on the performance of automotive thermoelectric generator. Energy Convers Manag 2016;126:266–77. doi:10.1016/j.enconman.2016.08.009.

[6] Lu C, Wang S, Chen C, Li Y. Effects of heat enhancement for exhaust heat exchanger on the performance of thermoelectric generator. Appl Therm Eng 2015;89:270–9. doi:10.1016/j.applthermaleng.2015.05.086.

[7] Amaral C, Brandão C, Sempels É V., Lesage FJ. Net thermoelectric generator power output using inner channel geometries with alternating flow impeding panels. Appl Therm Eng 2014;65:91–101. doi:10.1016/j.applthermaleng.2013.12.044.

[8] Ma T, Lu X, Pandit J, Ekkad S V., Huxtable ST, Deshpande S, et al. Numerical study on thermoelectric–hydraulic performance of a thermoelectric power generator with a plate-fin heat exchanger with longitudinal vortex generators. Appl Energy 2017;185:1343–54. doi:10.1016/j.apenergy.2016.01.078.

[9] Amaral C, Brandão C, Sempels É V., Lesage FJ. Thermoelectric power enhancement by way of flow impedance for fixed thermal input conditions. J Power Sources 2014;272:672–80. doi:10.1016/j.jpowsour.2014.09.003.

[10] Zhou S, Sammakia BG, White B, Borgesen P, Chen C. Multiscale modeling of Thermoelectric Generators for conversion performance enhancement. Int J Heat Mass Transf 2015;81:639–45. doi:10.1016/j.ijheatmasstransfer.2014.10.068.

[11] Aranguren P, Astrain D, Rodríguez A, Martínez A. Experimental investigation of the applicability of a thermoelectric generator to recover waste heat from a combustion chamber. Appl Energy 2015;152:121–30. doi:10.1016/j.apenergy.2015.04.077.

[12] Lu H, Wu T, Bai S, Xu K, Huang Y, Gao W, et al. Experiment on thermal uniformity and pressure drop of exhaust heat exchanger for automotive thermoelectric generator. Energy 2013;54:372–7. doi:10.1016/j.energy.2013.02.067.

[13] Aranguren P, Astrain D, Pérez MG. Computational and experimental study of a complete heat dissipation system using water as heat carrier placed on a thermoelectric generator. Energy 2014.

[14] Aranguren P, Astrain D, Martínez a. Study of Complete Thermoelectric Generator Behavior Including Water-to-Ambient Heat Dissipation on the Cold Side. J Electron Mater 2014;43:2320–30. doi:10.1007/s11664-014-3057-x.

[15] Shabgard H, Allen MJ, Sharifi N, Benn SP, Faghri A, Bergman TL. Heat pipe heat exchangers and heat sinks: Opportunities, challenges, applications, analysis, and state of the art. Int J Heat Mass Transf 2015;89:138–58. doi:10.1016/j.ijheatmasstransfer.2015.05.020.

[16] Reay DA, Kew PA, McGlen RJ. Heat pipes: Theory, design and applications. 6th ed. Waltham, MA: Butterworth-Heinemann: Elsevier; 2014.

[17] Brito FP, Alves A, Pires JM, Martins LB, Martins J, Oliveira J, et al. Analysis of a Temperature-Controlled Exhaust Thermoelectric Generator During a Driving Cycle. J Electron Mater 2016;45:1846–70. doi:10.1007/s11664-015-4258-7.

[18] Remeli MF, Date A, Orr B, Ding LC, Singh B, Affandi NDN, et al. Experimental investigation of combined heat recovery and power generation using a heat pipe assisted thermoelectric generator system. Energy Convers Manag 2016;111:147–57. doi:10.1016/j.enconman.2015.12.032.

[19] Singh R, Tundee S, Akbarzadeh A. Electric power generation from solar pond using combined thermosyphon and thermoelectric modules. Sol Energy 2011;85:371–8. doi:10.1016/j.solener.2010.11.012.

[20] Favarel C, Bédécarrats J-P, Kousksou T, Champier D. Experimental analysis with numerical comparison for different thermoelectric generators configurations. Energy Convers Manag 2015;107:114–22. doi:10.1016/j.enconman.2015.06.040.

[21] Angeline AA, Jayakumar J, Asirvatham LG, Marshal JJ, Wongwises S. Power generation enhancement with hybrid thermoelectric generator using biomass waste heat energy. Exp Therm Fluid Sci 2017;85:1–12. doi:10.1016/j.expthermflusci.2017.02.015.

[22] Weng C-C, Huang M-J. A simulation study of automotive waste heat recovery using a thermoelectric power generator. Int J Therm Sci 2013;71:302–9. doi:10.1016/j.ijthermalsci.2013.04.008.

[23] Aranguren P, Araiz M, Astrain D, Martínez A. Thermoelectric generators for waste heat harvesting : A computational and experimental approach. Energy Convers Manag 2017;148:680–91. doi:10.1016/j.enconman.2017.06.040.

[24] TG12-8-01L Power Generators | Generator Modules 2017. http://www.marlow.com/power-generators/standard-generators/tg12-8-01l.html (accessed September 17, 2017).

[25] Mavridou S, Mavropoulos GC, Bouris D, Hountalas DT, Bergeles G. Comparative design study of a diesel exhaust gas heat exchanger for truck applications with conventional and state of the art heat transfer enhancements. Appl Therm Eng 2010;30:935–47. doi:10.1016/j.applthermaleng.2010.01.003.

[26] Coleman HW, Steele WG. Experimentation, Validation, and Uncertainty Analysis for Engineers. 3rd ed. New Jersey: John Wiley & Sons; 2009.